International Journal of Applied Engineering Research
ISSN 0973-4562 Volume 9, Number 23 (2014) pp. 20509-20536

http://www.ripublication.com

Analysis of Gauss-Hermite Kalman Filter-Based Road Extraction Algorithms in Satellite Imagery

[1]K.Madhan Kumar, [2]R.Kanthavel, [3]A.Velayudham

[1]Associate Professor
Department of Electronics and Communciation Engineering,
PET Engineering College,Vallioor
madhankumar0879@gmail.com
[2]Professor Department of ECE,Vellammal Engineering College,Chennai
[3]Assistant Professor (S.G) Department of Information Technology
Cape Institute of Technology Levengipuram – 627114
Tirunelveli district

Abstract:

Road extraction from remotely sensed imagery is very practical for fast road updating in Geographic Information System (GIS) data collection. Recently, various methods proposed in the literature have met with only limited success due to complexity of accuracy. In order to bring more improvement, two different methods are proposed for road extraction from satellite images using Gauss-Hermite Kalman Filter. The ultimate aim of this paper is to perform a detailed analysis of road extraction methods such as i) Unscented Kalman Filter and Gauss-Hermite Kalman Filter-based, ii) S-Legion and GHKF-based, iii) LEGION-based, iv) Particle Filtering and Extended Kalman Filtering-based road extraction. The performances of four different road extraction algorithms are analyzed with different number of cluster given for seed point selection and to study the road extraction behavior of these algorithms. Here, five different evaluation metrics such as, sensitivity, specificity, accuracy, completeness and correctness are used as measurement metrics to measure the performance of algorithms in road extraction. Three satellite images are considered as test bed. From the experimental results, we ensure that the accuracy of Gauss-Hermite Kalman Filter-based proposed road extraction algorithm achieved better results when compared with existing algorithms.

1. Introduction

Network of roads is an indispensable means of transportation, and offers the backbone

for human civilization. Therefore, it is essential to preserve and restore roads to maintain our transportation network being linked. Roads generally appear as dark lines while observed from satellite images which are predominantly true in rural and sub-urban areas. Remote sensing data of the earth's surface is endlessly obtained from aircraft and spacecraft platform as it is readily existing in digital format [10]. Normally, the statistical models are employed to represent the traits of the road features. Here, these methods comprise two distinct stages: prediction stage and update stage. The technique based on the Extended Kalman Filter (EKF) is one of the best approaches in this class, which is employed for road map extraction in [11] and thereafter is again developed in [12] and [13]. Particle filters (PFs) are employed for nonlinear filtering. Algorithms based on PF have been employed in [14] and to trace a single road path initiated by a specified seed at the starting point of the road. Certain automatic initialization systems have been developed according to Geographical Information System (GIS) or geographical database which is reviewed in [13] and [15], and on heuristics [16], [11] or a stochastic assumption [14] [30].

Road network detection can be employed for various applications like mechanized correction and updating for geographic information systems (GIS) from aerial images [17], [18], registration with multi-temporal images for change detection [19]–[20], mechanically aligning two spatial datasets [21]–[22], etc. These applications not only necessitate detecting road networks but also must recognize road intersections [17], [21]. Of late, a number of literatures have been able to succeed only partially mainly on account of complexity of time and accuracy. To upgrade road-extraction accuracy, geometrical features of road have been investigated to incorporate them with spectral information. Dell'Acqua and Gamba [23] employed the fuzzy Hough transform to recognize linear features. Song and Civco [24] integrated shape features with pixel wise support vector machine classification outcome to extract road. Shi and Zhu [25] developed to mine road from a binary map by means of the line segment match technique. Although incorporating shape features and spectral feature yield a superior performance, it is hard to obtain a universal linear-feature-extraction technique for any condition [26], and supplementary studies are highly essential. In the course of the road-extraction procedure, immediately when the potential road segments are gathered, a thinning algorithm is usually executed to mine road centerlines [24]. Anyhow, the centerlines gathered from thinning algorithms have several spurs which curtail the smoothness of the centerline. Smooth-road-centerline extraction should be subjected to supplementary investigation.

A number of literatures have tried to find a solution to the issue of road extraction from satellite images [5, 6, and 7]. In Alharthy and Bethel [5], the points were filtered by their intensity, proximity to a digital terrain model (DTM) and thereafter the network was mined by locating linked modules. Clode *et al*. [7] make use of an identical method to choose candidate road points. Anyhow, instead of employing a linked module filter they mine the road area by using a phase coded disk operator [7] and continue with joining and intersecting the extracted roads. In Choi *et al*. [6], road points were mined by a sequence of circle buffers clustering points by elevation and reflectance and integrating clusters in accordance with the greatest possible slope of the road. Conversely, certain experiences detailed in [8]–[9] point out that, on

account of the deficiency of strength of automatic extraction tools, the finest method to step up the productivity lies in scheming semi-automatic tools. If an automatic process is prone to fail, the most excellent method is to allow the operator gain full control of the process, instead of obliging this operator to look for the inaccurate outcomes on the entire image. Hence, when take into consideration all the above problems; it is high time a proficient road extraction is launched to tackle this ticklish issue.

2. Description of the Chosen Road Extracton Algorithms

The ultimate target of the proposed research is to compare the road extraction algorithms explained in the literature [1, 2, 3 and 4]. Algorithms developed to perform road extraction using satellite images are selected for comparison. To effectiveness of comparative analysis, we compare our GHKF based proposed algorithms [1] [2] with S.Movaghati *et al*. [4] algorithm and Jiangye Yuan *et al.* [3] algorithm. The following subsections provide a detailed explanation of the tracking process of considered road extraction algorithms.

2.1. Our Previous algorithm [1]

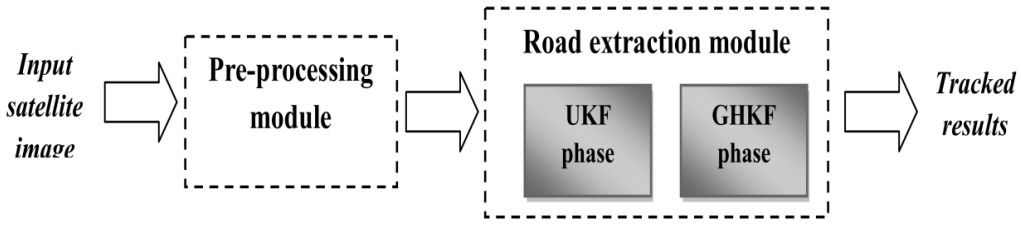

Fig 1: Overall block diagram of our previous road extraction algorithm [1]

As illustrated in figure 1, our previous system [1] is divided into following two important modules:

a. Automatic road region selection (preprocessing module)

The preprocessing module consists of two modules. At first, the reference road model is manually generated. This road model is taken from input original satellite image. Secondly, the seed point selection is done by grid based clustering. Here, road extraction process starts from this seed point i.e. initialization point. Finally, the Unscented Kalman filter and Gauss-Hermite Kalman Filter are used for the road extraction process.

Seed point selection using grid based clustering:

The seed point selection is done by grid based clustering. Road extraction process

starts from this seed point i.e. initialization point. K-means algorithm is used to identify the initial point of the road from the satellite image. The significant process of seed point selection is described below:

1) Create the grid structure of the satellite image.
2) Each grid pixel values are arranged into row format based on the grid structure.
3) Applying k-means algorithm [29] utilized in road extraction in satellite image for the selection of the initial point of the road which has traced path then calculates the minimum distance based on the following objective function.

$$J = \sum_{i=1}^{k} \sum_{j=1}^{n} \left\| x_j^{(i)} - c_i \right\|^2 \quad (1)$$

Where, $\left\| x_j^{(i)} - c_i \right\|^2$ is a chosen distance measure between a data point $x_j^{(i)}$. c_j is the cluster center.

4) For k-means clustering process, firstly k initial (in this technique $k = 10$) are randomly generated within satellite image.
5) K-clusters are generated by associating every observation with the nearest mean.
6) The centroid of each of the k-clusters becomes the new mean.
7) Steps 5 and 6 are repeated until convergence has been reached.
8) The reference profile is matched with each cluster; one less distance segment is obtained using Euclidean distance.
9) Again, this less distance cluster is matched with grid profile, finally, we obtain one less distance cluster or road segment using Euclidean distance. From this segment, we start the road tracing procedure.

b. Road prediction traverse model using UKF and corrective road path chosen using GHKF

- **UKF phase:**

This phase is initialized with a seed point given at the starting of the road extraction process. The beginning point contains coordinates of the road center and direction of the road at that point. The road center coordinates and road direction are considered as the initial state of the proposed system, called y_1. This starting point is employed to initialize the grid based clustering technique. The UKF phase begins tracking the road using starting start and initial grid based cluster.

When the UKF phase visits a severe obstacle on the road path or arrives at a road junction, the matching process cannot successfully generate next prediction state. An update profile is extracted from the observation model. This profile is compared with reference profile. In this stage, we have assigned some predefined threshold for the road region, and this threshold is based on the RGB image. If the prediction is above the threshold and the UKF stops and passes the control to the GHKF phase. In this case, the GHKF makes another state update based on the current position, so as the estimation position is jumped over. When multiple jumps occurs, the Gauss-Hermite Kalman Filter identifies it as a tracking failure and return control back to the Unscented Kalman Filter.

Prediction stage:

We first choose, M sample points $Y^i_{|q-1}$ and their weights $w^i_{|q-1}$, i=0, 1…N-1. These sample points capture the true mean and covariance of the density function and hence approximate the true density function up to the second order statistics.

$$Y^i_{q|q-1} = f(y^i_{q-1|q-1}) \quad (2)$$

These samples denotes the predicted density $p(x_{q|z-1})$ and its means and covariance is given by

$$\hat{y}_{q|q-1} = \sum_{i=0}^{N-1} w_i Y^i_{q|q-1} \quad (3)$$

$$P_{q|q-1} = \sum_{i=0}^{N-1} w_i [Y^i_{q|q-1} - \hat{y}_{q|q-1}][Y^i_{q|q-1} - \hat{y}_{q|q-1}]^T \quad (4)$$

Therefore, $p(x_q|z-1)$ is estimated by assuming that is distributed as $N(\hat{x}_{q|q-1,}P_{q|q-1})$ at the end of the prediction stage. Then, the predicted measurement vector is calculated as below:

$$\hat{z}_{q|q-1} = \sum_{i=0}^{N-1} w_i h(Y^i_{q|q-1}) \quad (5)$$

After prediction stage, all predictions have gone to be updated using the observation obtained in the q^{th} step, called z_q.

Update stage:

$$\hat{y}_{q|q} = \hat{y}_{q|q-1} + K_q(z_q - \hat{z}_{q|q-1}) \quad (6)$$

$$P_{q|q} = P_{q|q-1} - K_q S_q K_q^T \quad (7)$$

Here, K_q is the kalman gain and S_q innovation covariance matrices and these are computed as following formulas:

$$K_q = P_{uv} S_q^{-1} \quad (8)$$

$$S_q = R_q + P_{vv} \quad (9)$$

Where

$$P_{uv} = \sum_{i=0}^{N-1} w_i (Y^i_{q|q-1} - \hat{y}_{q|q-1})(h(Y^i_{q|q-1}) - \hat{z}_{k|k-1})^T$$

$$P_{vv} = \sum_{i=0}^{N-1} w_i (Y^i_{q|q-1} - \hat{z}_{q|q-1})(h(Y^i_{q|q-1}) - \hat{z}_{k|k-1})^T$$

- **GHKF phase:**

To initialize the GHKF phase, the UKF phase relocates the information about its last successful step of the present road segment onto the GHKF phase. The GHKF begins its work with a single road branch by using the last successful state estimate of the UKF phase as its initial state y_1 .

Prediction stage:

- Calculate the root $y_i, i = 1,... p$, of the Hermite polynomial $H_p(y)$.
- Calculate the corresponding weights

$$w_i = \frac{2^{p-1} p!}{p^2 [H_{p-1}(y_i)]^2} \quad (10)$$

- Use the product rule to expand the points to a n dimensional lattice of p^n points $\xi_i, i = 1,..., p^n$, with corresponding weights.
- Propagate the cubature points. The matrix square root is the lower triangular cholesky factor.

$$Y_{i,q-1|q-1} = \sqrt{2P_{q-1|q-1}}\,\xi_i + m_{q-1|q-1} \quad (11)$$

- Evaluate the cubature points with the dynamic model function

$$Y^*_{i,q|q-1} = f(Y_{i,q-1|q-1}) \quad (12)$$

- Estimate the predicted state mean

$$m_{q|q-1} = \sum_{i=1}^{p^n} w_i Y^*_{i,q|q-1} \quad (13)$$

- Estimate the predicted error covariance

$$P_{q|q-1} = \sum_{i=1}^{p^n} w_i Y^*_{i,q|q-1} Y^T_{i,q|q-1} - m_{q|q-1} m_{q|q-1}{}^T + Q_{q-1} \quad (14)$$

2.1. Our Proposed algorithm [2]

To improve the road extracted results of our previous algorithm [1], in this paper, we have proposed an efficient road extraction algorithm using S-LEGION and GHKF. Before the road extraction process, some enhancement process is done by preprocessing stage. The overall block diagram of proposed road extraction algorithm is illustrated in figure 2.

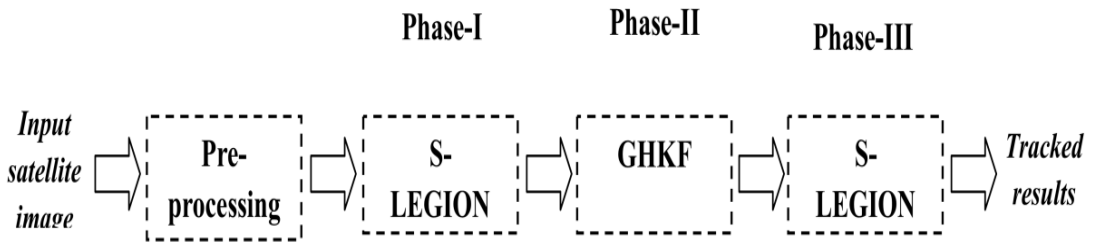

Fig 2: Overall block diagram of our proposed algorithm [2]

(i) Preprocessing:
At first, the input satellite images are preprocessed to remove the noises present in the images and to make the images suitable for further processing. Here, pre-processing is done through i) contrast adjustment (ii) morphological operation iii) Laplace filter.

(ii) Initial leader selection:
A seed point is the starting point for road extraction process and its selection is very vital to the road tracking results. Many existing methods start with the selection of seed point provided by the user. In our algorithm, we have developed an automatic seed point selection method to extract the road from the satellite image. At first, a reference road model (M_1) with size of 11×11 is manually generated to help initial leader point selection. Then, an initial leader point is generated by matching the reference model with each of the pixel in the satellite image. Here, k-means algorithm is used for this purpose.

(iii) PHASE I: S-LEGION
To improve the LEGION process, in this section we have proposed a method, called S-LEGION, an automatic seed point selection with LEGION based road extraction method from the satellite image. The seed point selection is explained in section (ii). This method has two phases namely silent phase and the active phase, the medial points oscillates between the silent and active phase during the process. The proposed S-LEGION based road extraction of satellite images involves several stages such as:

- **Stage 1**: Initialization
- **Stage 2**: Self excitable cell detection
- **Stage 3**: Self excitation
- **Stage 4**: Excitable cell detection
- **Stage 5**: Excitation of dependent cell
- **Stage 6**: Inhibition

(iv) PHASE II: GAUSSIAN HERMIT KALMAN FILTER
In this phase, a non-linear filter is used to extract the remaining road from the satellite

image. To initialize the GHKF phase, the S-LEGION phase relocates the information about its last successful step of the present road segment onto the GHKF phase. The GHKF begins its work with a single road branch by using the last successful state estimate of the S-LEGION phase as its initial state y_1 .

Prediction stage:

- Find the root $y_i, i = 1,...p$, of the Hermite polynomial $H_p(y)$.
- Compute the corresponding weights

$$w_i = \frac{2^{p-1} p!}{p^2 [H_{p-1}(y_i)]^2} \quad (15)$$

- Use the product rule to expand the points to a n dimensional lattice of p^n points $\xi_i, i = 1,..., p^n$, with corresponding weights.
- Propagate the cubature points. The matrix square root is the lower triangular cholesky factor.

$$Y_{i,q-1|q-1} = \sqrt{2P_{q-1|q-1}}\,\xi_i + m_{q-1|q-1} \quad (16)$$

- Evaluate the cubature points with the dynamic model function

$$Y^*_{i,q|q-1} = f(Y_{i,q-1|q-1}) \quad (17)$$

- Estimate the predicted state mean

$$m_{q|q-1} = \sum_{i=1}^{p^n} w_i Y^*_{i,q|q-1} \quad (18)$$

- Estimate the predicted error covariance

$$P_{q|q-1} = \sum_{i=1}^{p^n} w_i Y^*_{i,q|q-1} Y^T_{i,q|q-1} - m_{q|q-1} m_{q|q-1}{}^T + Q_{q-1} \quad (19)$$

Update stage:

1. Repeat steps 1-3 from earlier to get the p^n cubature points and their weights.
2. Propagate the cubature points.

$$X_{i,k|k-1} = \sqrt{2P_{k|k-1}\xi_i} + m_{k|k-1} \quad (20)$$

3. Evaluate the cubature points with the help of the measurement model function

$$Y_{i,k|k-1} = h(X_{i,k|k-1}) \quad (21)$$

4. Estimate the predicted measurement

$$\hat{y}_{k|k-1} = \sum_{i=1}^{p^n} w_i Y_{i,k|k-1} \quad (22)$$

5. Estimate the innovation covariance matrix

$$S_{k|k-1} = \sum_{i=1}^{p^n} w_i Y_{i,k|k-1} Y_{i,k|k-1}{}^T - \hat{y}_{k|k-1} \hat{y}_{k|k-1}{}^T + R_k \quad (23)$$

6. Estimate the cross-covariance matrix

$$P_{xy,x|k-1} = \sum_{i=1}^{p^n} w_i X_{i,k-1|k-1} Y_{i,k|k-1}{}^T - m_{k|k-1} \hat{y}_{k|k-1}{}^T \quad (24)$$

7. Calculate the Kalman gain term and the smoothed state mean and covariance

$$K_k = P_{xy,k|k-1} S_{k|k-1}^{-1} \quad (25)$$

$$m_{k|k} = m_{k|k-1} + K_k (y_k - \hat{y}_{k|k-1}) \quad (26)$$

$$P_{k|k} = P_{k|k-1} - K_k P_{yy,k|k-1} K_k^T \quad (27)$$

(v) PHASE III: S-LEGION

In final phase, if any road region cannot extract through first two phases, again phase-3 will continue the tracing process using S-LEGION. In this phase, leader is selected through reference model-2 (M_2). The new leader selection is done by following process:

- At first, Euclidean distance between reference model-2 (M_2) and whole image (I_i) to find the new leader pixel for road extraction. The Euclidean distance is calculated for every (11×11) pixel in the original image or (whole image). The new leader is selected as figure 7.

$$Ed_3 = \sum_{R_i, G_i B_i = 1}^{N} \sqrt{\frac{(R_i^2 - RI_i) + (G_i^2 - GI_i) + (B_i^2 - BI_i)}{3}} \quad (28)$$

Where, R_i^2 → indicates i^{th} pixel point of reference model-2 (for R component)

RI_i → indicates i^{th} pixel point of whole image I_i

G_i^2 → indicates i^{th} pixel point of reference model-2(for G component)

GI_i → indicates i^{th} pixel point of whole image I_i

B_i^2 → indicates i^{th} pixel point of reference model-2 (for B component)

BI_i → indicates i^{th} pixel point of whole image I_i

- From the above minimized pixel, the remaining and completing road extraction process is performed.

2.3. Jiangye Yuan et al. algorithm [3]

Jiangye Yuan *et al*. [3] have developed an automatic method for road extraction from satellite imagery using LEGION dynamics. The overall block diagram of the Jiangye Yuan *et al*. algorithm [3] is depicted in figure 3.

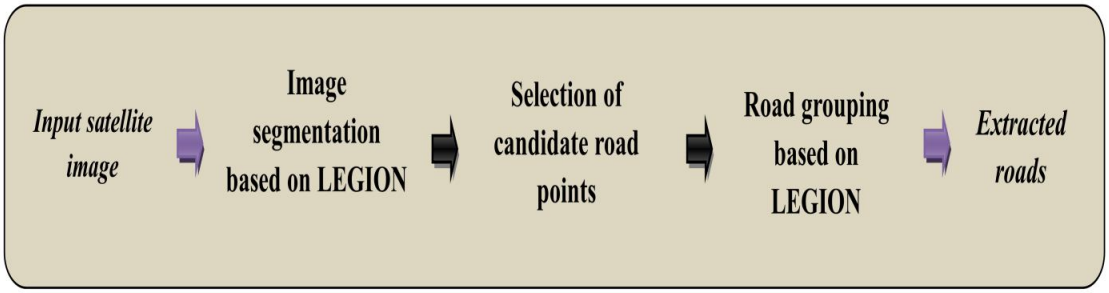

Fig 3: Overall block diagram of Jiangye Yuan *et al*. algorithm

As illustrated in figure 3, the road extraction task is decomposed into following three stages.

a. Image segmentation using a LEGION network

In this section, image segmentation is performed by locally excitatory globally inhibitory oscillator Networks (LEGION). LEGION is a system of D. Terman and Wang [27] to assemble traits of an object and segment diverse objects by means of oscillatory correlation. Each oscillator is designed as a standard relaxation oscillator. Local excitation is executed by positive coupling between neighbouring oscillators and global inhibition is attained by a global inhibitor. LEGION exhibits the mechanism of selective gating, in which oscillators inspired by the identical models tend to harmonize in view of the local excitation and oscillator groups motivated by various models tend to desynchronize owing to global inhibition. Such an oscillator is termed as a leader. A key oscillator block has to comprise at least one leader, while a noisy fragment suffers from the deficiency of a leader. In the segmentation task, leaders are encouraged to activate oscillator groups. All the fragments matching with oscillators that are unable to sustain oscillations and are therefore treated as background. In short, segmentation is accomplished in two stages. The former step is meant for regions and it generates huge and smooth segments. The latter step is planned to be susceptible to boundaries which show a tendency of being missed in the former step, and the latter step segments thin the area with clear edges.

b. Medial axis extraction within each segment and selection of points located in potential road areas

Once the segmentation of an image is over, the segments related to roads should be chosen. The medial axis transform is used to attain this target [28]. A general method to estimate the medial axis is the Voronoi diagram. A closing operation is at first executed to even the boundary-closing and is described as a dilation operation in which every background pixel adjacent to an object pixel is transformed into an object pixel, followed by an erosion operation in which every object pixel adjacent to a background pixel is transformed into a background pixel. By taking the boundary pixels of segments as the samples, the medial axis points of every segment are gathered from the Voronoi diagram. Every medial axis point with its radius shows the

location and dimension of the region in which it lies. As road regions are pigeonholed by their narrow widths, a medial axis point is chosen as a candidate if its radius is satisfactorily small. The radius threshold is estimated by image resolution and target road width. Medial axis points are chosen in place of segments as there are segments which partly belong to roads owing to segmentation error, and consequently, choice based on medial axis points offers further precise outcomes.

c. Road medial axis point grouping using a LEGION model with alignment dependent connections

Once the selection is made, the medial axis points matching with roads are mainly mined. Any hos, there are non-road points which are also chosen in view of their small radii. With a view to cluster road points and do away with non-road points, a LEGION model with alignment-dependent connections is launched. By LEGION dynamics, oscillators analogous to the medial axis points of one road are synchronized, and those matching with the medial axis points of various roads are desynchronized. The oscillators which are not sufficiently aligned with any of the leaders continue to be excitable during the procedure. Consequently, the medial axis points signifying roads are mined. The mined points have a dense allocation, leading to road centerlines. According to the mined points, the road regions can be effortlessly restored. A pixel is branded as a road region if it is in the identical section to the medial axis point and within the circle demarcated by the radius recorded at that point.

The choice phase generates certain medial axis points matching with road like objects, e.g., sidewalks and trees, along road sides. As they are in neighbourhood and parallel to roads, they may be clustered into the resultant roads. With a view to eliminate those non-road points, the sign that roads have distinct gray value is integrated into the clustering phase. When a leader in road regions is inspired, it tends to enlist the oscillator with an analogous pixel value, in which the threshold is the identical to that obtained in the step of achieving road segments.

2.4. S. Movaghati et al. algorithm [4]

S. Movaghati *et al*. [4] have presented a road tracking algorithm combining Extended Kalman Filter (EKF) with a special particle filter (PF) in order to regain the trace of the road beyond obstacles, as well as to find and follow different road branches after reaching to a road junction. The road-tracking algorithm comprises two crucial modules: the EKF module and the PF module. These two modules alternately transfer the command of the task to each other, as detailed in the ensuing two sections. Figure 4 shows the overall procedure of the Movaghati *et al*. [4] road-tracking algorithm.

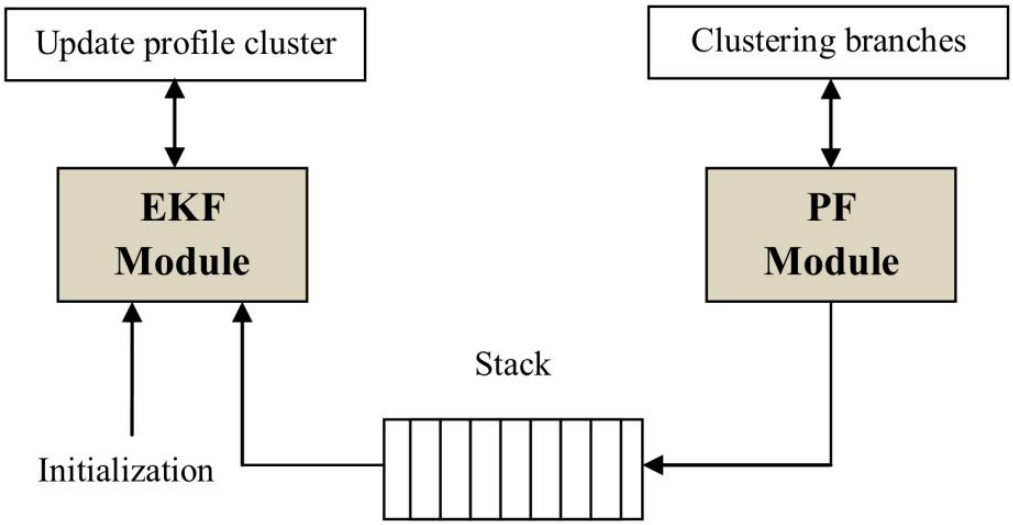

Fig 4: Overall block diagram of S. Movaghati *et al*. algorithm

a. EKF module

This module is initialized with a seed point specified at the commencement of the road-tracking process. The beginning point should embrace coordinates of the road center, road direction, and a coarse estimation of the road width at that point. The road center coordinates and the road direction are construed as the initial state of the mechanism, viz, x_1 (the fourth element of x_1 is presumed to be zero). The relative beginning point is also employed to initialize the profile cluster.

The EKF module begins with tracking the road by means of the initial state and the initial profile cluster. In the course of progress along the road path, the profile clusters are revised, and fresh suitable clusters are supplemented as road intensities and/or widths change. When the EKF module is thrown open to a ruthless obstacle on the road path or reaches a road junction, the update profile cluster process is incompetent to produce fresh profile clusters. This arises out of the fact that the profiles mined at road junctions or obstacles fail to pass corroboration tests or survive the validation procedure after a given number of steps from their formation. Hence, the moving average of the profile error tends to go up and go beyond a specified threshold. This threshold decides the place where the EKF module should end. This threshold can have a sway over the entire result of the road detection algorithm. If it is assigned a very insignificant value, the EKF module tends to come to end very frequently at every minor obstacle or noise on the road path. Conversely, a very lofty threshold value tends to trigger the EKF algorithm to move into an erroneous off-road area or pass over a junction without locating road branches.

a. PF module

Subsequently, without effecting termination of the procedure, the outcomes are passed on to the PF algorithm which tends to locate the continuance of the road after a potential obstacle or to recognize all probable road branches that may be there on the opposite side of a road junction. With a view to get added perfection, we have customized the process for getting the dimensions by decoupling this procedure from the current state prediction of the filter. Doing away with the reliance of the dimension data to the predicted state scales down the possibility for unsteadiness of the road-tracing algorithm. Moreover, we have devised a technique for dynamic clustering of the road profiles so as to preserve tracing when the road profile is subjected to certain alterations on account of changes in the road width and intensity.

3. Experimental Setup

The proposed comparative analysis is performed in a windows machine having configurations Intel (R) Core i5 processor, 3.20 GHz, 4 GB RAM, and the operating system platform is Microsoft Wnidow7 Professional. We have used mat lab latest version (7.12) for this proposed analysis.

3.1. Dataset description

The proposed comparative analysis was tested on three different satellite images, these are collected through internet. Both images represent urban environment and are illustrated in figure 4. The input image size is 1200 by 900 pixels.

4(a) **4(b)** **4(c)**

Fig 4: Input Satellite images

3.2. Evaluation matrices

The results are evaluated using important evaluation matrices called sensitivity, specificity and accuracy, completeness and correctness. The evaluation of proposed comparative analysis in three satellite images are carried out using the following metrics as suggested by below equations (29) to (33),

$$Sensitivity = \frac{TP}{TP + FN} \tag{29}$$

$$Specificity = \frac{TN}{TN + FP} \quad (30)$$

$$Accuracy = \frac{TN + TP}{TN + FP + FN + TP} \quad (31)$$

$$Completeness = \frac{TP}{TP + TN} \quad (32)$$

$$Correctness = \frac{TP}{TP + FN} \quad (33)$$

Where, TP stands for True Positive, TN stands for True Negative, FN stands for False Negative and FP stands for False Positive. ***Sensitivity*** is the proportion of true positives that are correctly identified by a proposed method. It shows how good the test is at detecting a road. ***Specificity*** is the proportion of the true negatives correctly identified by proposed method. It suggests how good the test is at identifying normal (negative) condition. ***Accuracy*** is the proportion of true results, either true positive or true negative, in a population. Completeness

3.3. Experimental results

This section describes the experimental results and comparative analysis of four considered algorithms. These algorithms are implemented using MATLAB. Here, for comparison, we have taken three satellite image shown in figure 4. The overall proposed road extraction algorithm provides the results in figures 5 to 8 for three test areas. Figure 5 illustrates the road extraction results of S.Movaghati *et al.* algorithm [4] of three test satellite images. Figure 6 shows the road extraction results of Jiangye Yuan *et al.* algorithm [3] for three test images. Figure 7 depicts the road extraction our previous technique [1] for three test images. GHKF based proposed algorithm results for three test images are shown in figure 8.

5a

5b

5c

Fig 5: Road extraction results of S.Movaghati *et al.* algorithm [4] for three test images

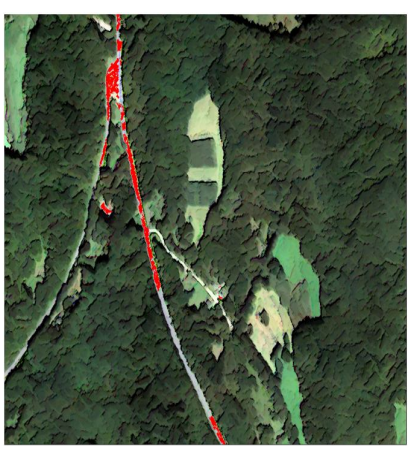

6a

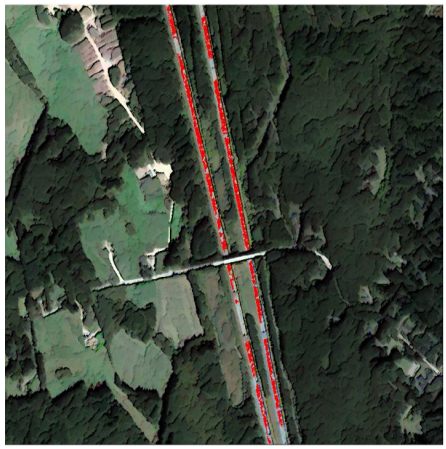

6b

6c

Fig 6: Road extraction results of Jiangye Yuan *et al.* algorithm [3] for three test images

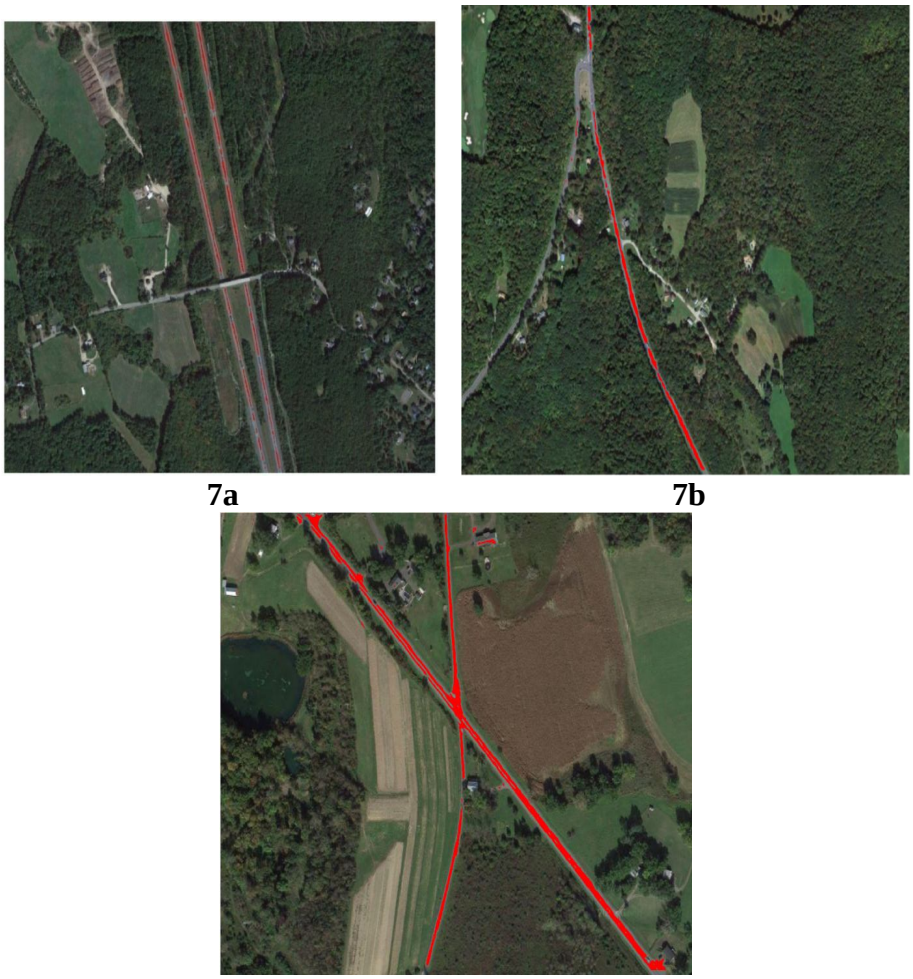

7a **7b**

7c

Fig 7: Road extraction of our previous technique [1] for three test images

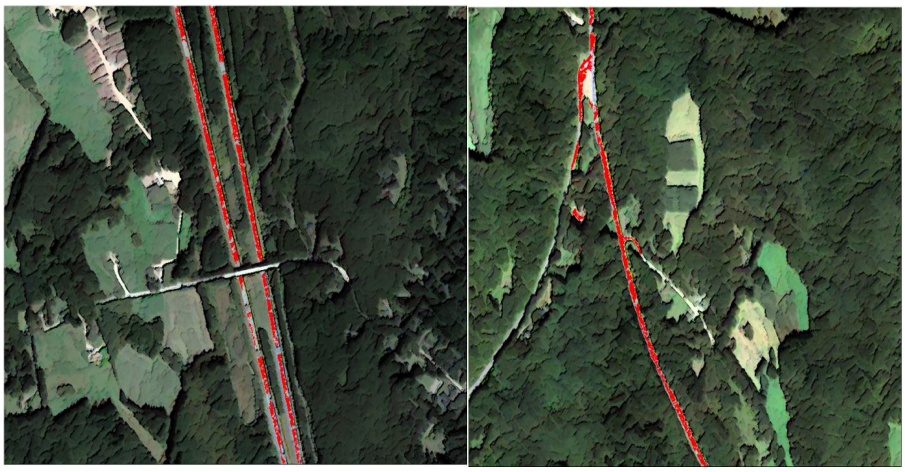

8a **8b**

8c

Fig 8: Road extraction results of our proposed technique [2] for three test images

3.4. Quantitative analysis

The robustness of the considered road extraction algorithms can be evaluated with the help of five evaluation matrices like as accuracy, completeness, correctness, sensitivity and specificity.

To evaluate the performance of our proposed approach, we compare our two GHKF based road extraction results [2] and [1] with other two road extraction methods such as S.Movaghati *et al.* [4] algorithm and Jiangye Yuan *et al.* [3] algorithm. The performances of the road extraction results are shown in figure 9 to 23 for three satellite images. Following subsection explains the performance of the considered algorithms using five evaluation matrices.

3.4.1. Accuracy

The accuracy of the considered algorithms is calculated for different number of cluster in proposed comparative analysis. The obtained accuracy values for different algorithms are plotted as a graph shown in figure 9, 10 and 11 for three satellite images. According to figure 9, our proposed algorithm [2] or Gauss-Hermite Kalman filter (GHKF)-based road extraction algorithm [2] is achieved the accuracy of about 98.30% in cluster 10, 98.25% in cluster 15, 98.30% in cluster 20 where, S.Movaghati *et al.* [4] algorithm has achieved only 97.62% in cluster 10, 97.64% in cluster 15, 97.76% in cluster 20. At the same time, Jiangye Yuan *et al.* [3] algorithm achieved only 98.26% in cluster 10, 98.25% in cluster 15, 98.26% in cluster 20. On other hand, another GHKF based road extraction algorithm [1] (our previous algorithm) attained better results when compared with S.Movaghati *et al.* [4] algorithm.

In figure 10, our proposed algorithm [2] is achieved the accuracy of about 98.46% in cluster 10, 98.29% in cluster 15, 98.48% in cluster 20 where S.Movaghati *et al.* [4] algorithm has achieved only 97.95% in cluster 10,97.64% in cluster 15,97.76% in cluster 20 and Jiangye Yuan *et al.* [3] algorithm achieved only 98.44% in cluster 20. In figure 11, our proposed GHKF based road extraction algorithm [2] is attained the

accuracy of about 97.63% in cluster 15, 97.70% in cluster 20 but S.Movaghati *et al*. [4] algorithm has achieved only 96.33% in cluster 10, 96.49% in cluster 20 and Jiangye Yuan *et al.* [3] algorithm achieved only 97.50% in cluster 15, 97.56% in cluster 20. Totally, analyzing figures 9, 10 and 11, our GHKF based road extraction algorithm achieved better accuracy when compared with S.Movaghati *et al*. [4] algorithm and Jiangye Yuan *et al.* [3] algorithm.

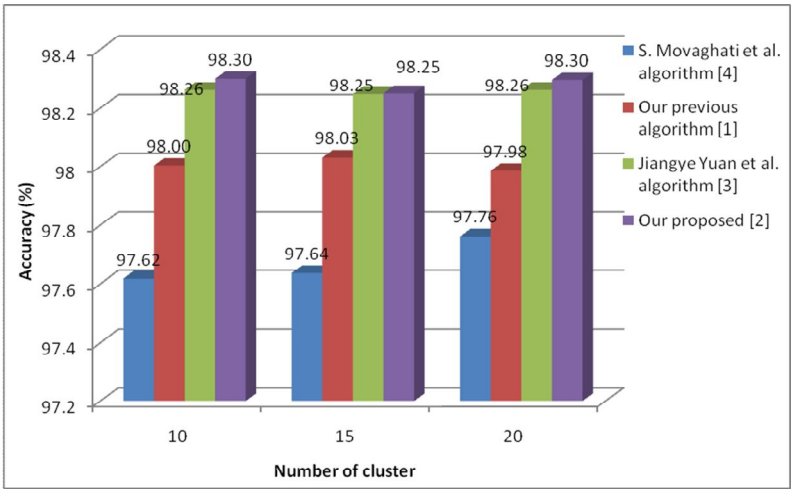

Fig 9: Accuracy plot of comparative analysis for image 1

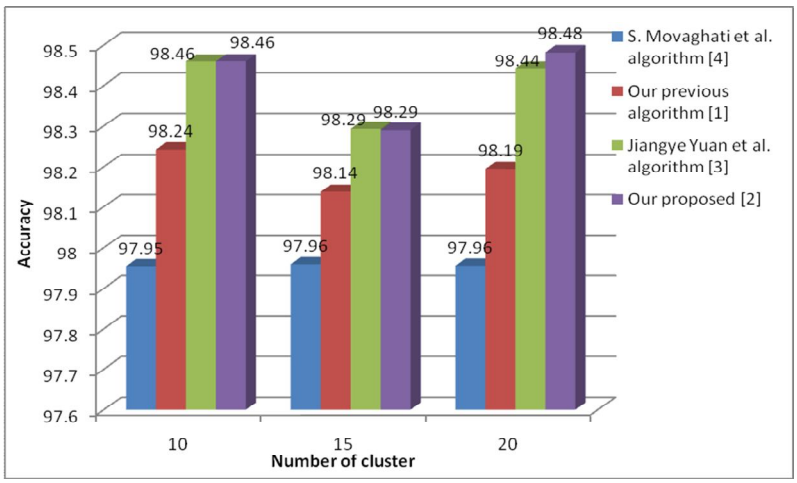

Fig 10: Accuracy plot of comparative analysis for image 2

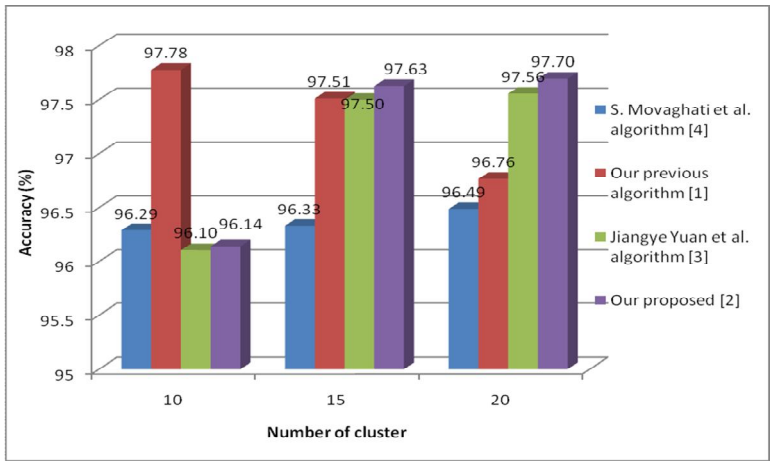

Fig 11: Accuracy plot of comparative analysis for image 3

3.4.2. Completeness

The comparison of considered road extraction algorithms based on completeness is given in this subsection. The completeness values are computed for different number of cluster in proposed comparative analysis and the values are plotted in figure 12, 13 and 14 for the considered algorithms. According to figures (image 1), our proposed algorithm [2] or Gauss-Hermite Kalman filter-based road extraction algorithm [2] is achieved the completeness of about 98.89% in cluster 10, 98.78% in cluster 15, 98.86% in cluster 20 where, S.Movaghati *et al*. [4] algorithm has achieved only 97.97% in cluster 10,98.07% in cluster 15,98.30% in cluster 20 and Jiangye Yuan *et al.* [3] algorithm achieved only 98.80% in cluster 10, 98.78% in cluster 15, 98.80% in cluster 20. Totally, analyzing figure 12, 13 and 14, the GHKF based road extraction algorithm is better performance when compared with others like as Extended Kalman Filter (EKF) and LEGION based road extraction algorithms.

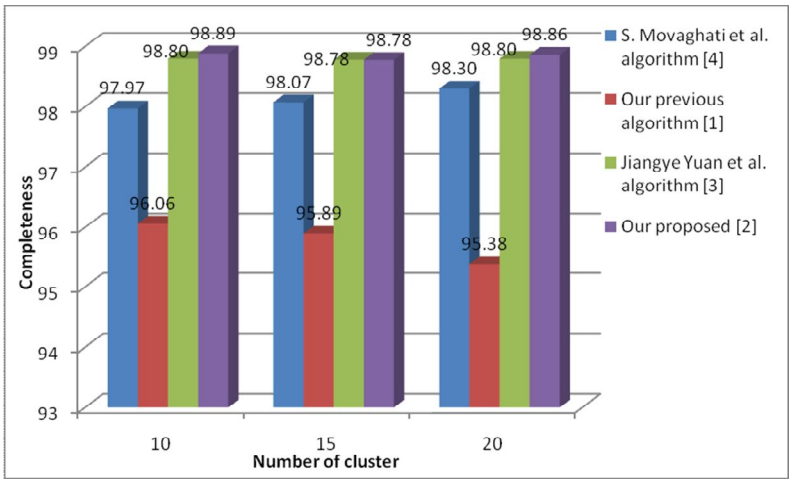

Fig 12: Completeness plot of comparative analysis for image 1

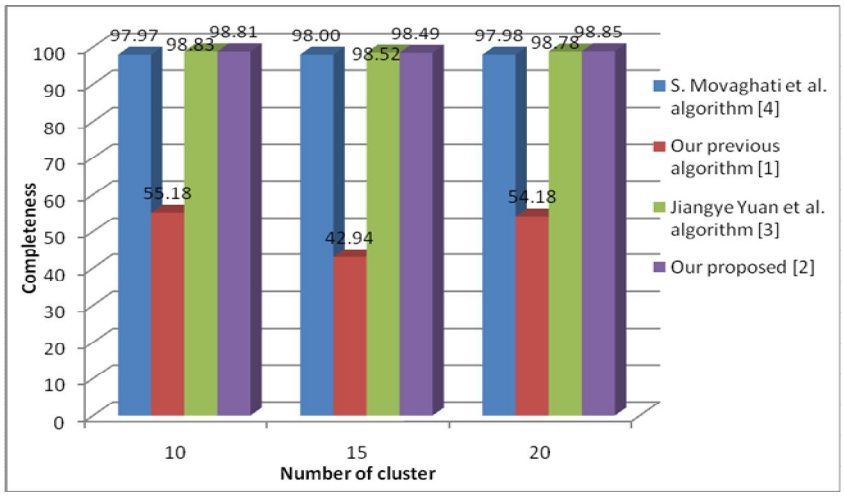

Fig 13: Completeness plot of comparative analysis for image 2

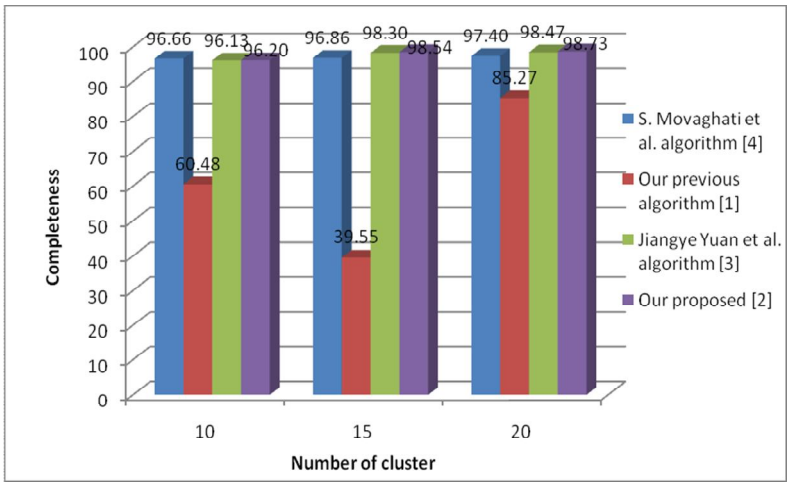

Fig 14: Completeness plot of comparative analysis for image 3

3.4.3. Correctness

The correctness of the considered algorithms is calculated for various numbers of clusters in proposed comparative analysis. The obtained correctness values for different algorithms are plotted in figure 15, 16 and 17. Analyzing the graphs, in image 2, our Gauss-Hermite Kalman filter (GHKF)-based road extraction algorithm [2] is achieved the correctness of about 96.50% in cluster 10, 96.41% in cluster 15, 96.56% in cluster 20 where, S.Movaghati *et al*. [4] algorithm has achieved only 95.99% in cluster 10, 95.99% in cluster 15, 95.99% in cluster 20. At the same time, Jiangye Yuan *et al.* [3] algorithm achieved only 96.49% in cluster 10, 96.41% in cluster 15, 96.51% in cluster 20. Thoroughly, analyzing figure 15, 16 and 17, the correctness performance is better results in our GHKF based road extraction algorithm when compared with other algorithms.

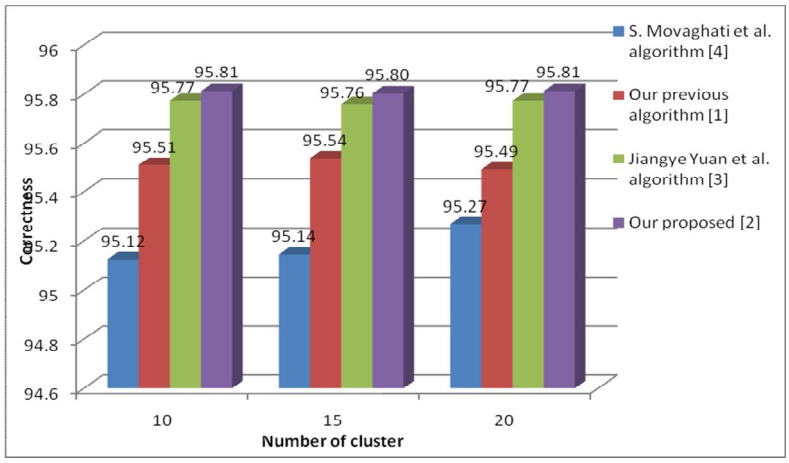

Fig 15: Correctness plot of comparative analysis for image 1

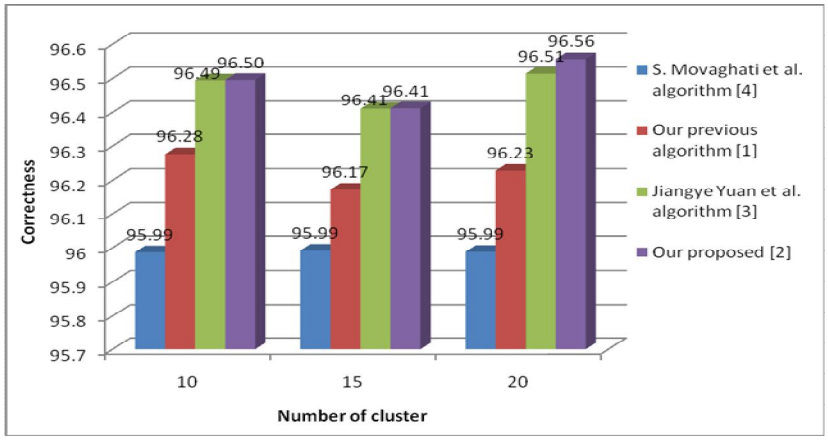

Fig 16: Correctness plot of comparative analysis for image 2

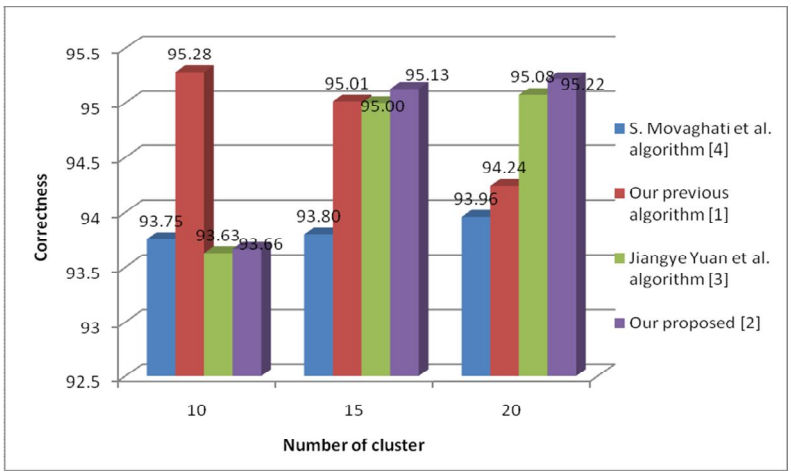

Fig 17: Correctness plot of comparative analysis for image 3

3.4.4. Sensitivity

The comparison of considered road extraction algorithms based on sensitivity is given in this subsection. The sensitivity values are computed for different number of cluster in proposed comparative analysis and the values are plotted in figure 18, 19 and 20 for the considered algorithms. According to figures, in figure 3, our Gauss-Hermite Kalman filter-based road extraction algorithm [2] is achieved the sensitivity of about 37.79% in cluster 15, 39.87% in cluster 20 where, S.Movaghati *et al.* [4] algorithm has achieved only 2.89% in cluster 15, 7.27% in cluster 20 and Jiangye Yuan *et al.* [3] algorithm achieved only 34.31% in cluster 15, 36.12% in cluster 20. Totally, analyzing figure 12, 13 and 14, the sensitivity performance is better for GHKF based road extraction algorithm when compared with others like as Extended Kalman Filter (EKF) and LEGION based road extraction algorithms.

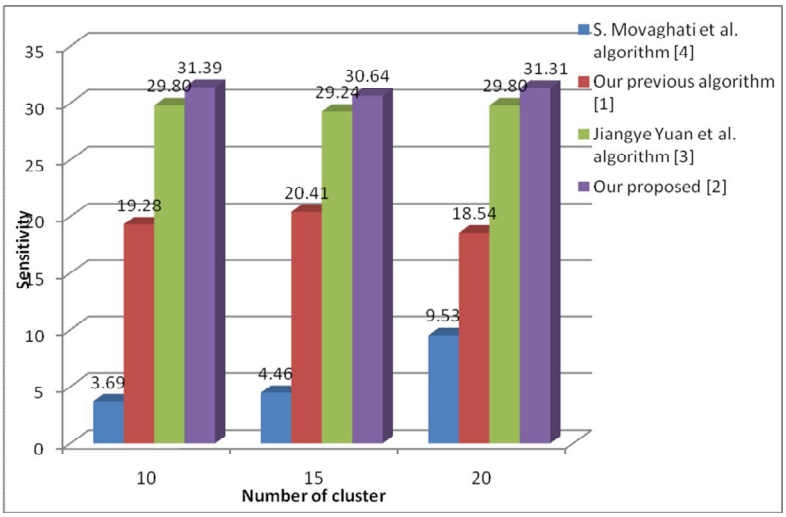

Fig 18: Sensitivity plot of comparative analysis for image 1

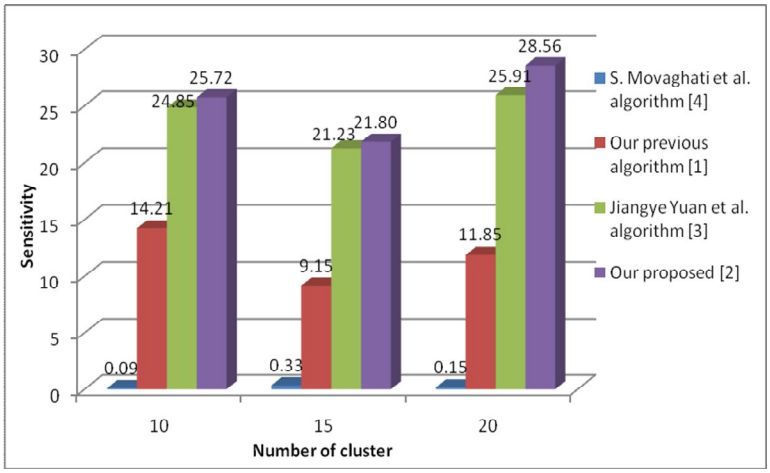

Fig 19: Sensitivity plot of comparative analysis for image 2

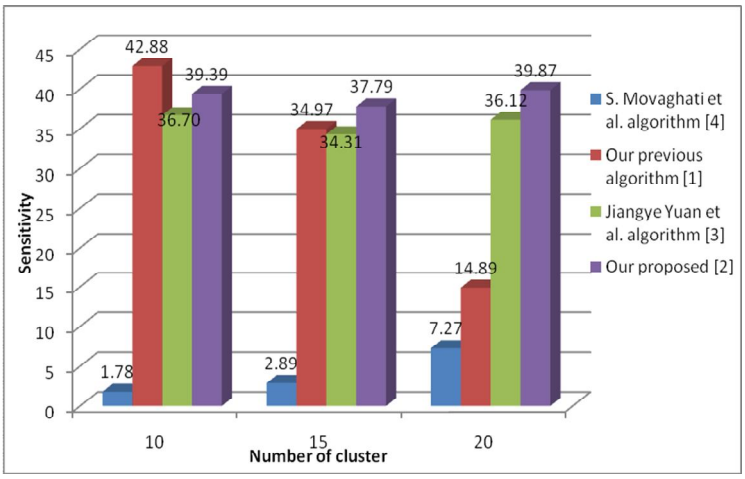

Fig 20: Sensitivity plot of comparative analysis for image 3

3.4.5. Specificity

The specificity of the considered road extraction algorithms is computed for various numbers of clusters in proposed comparative analysis. The obtained specificity values for different algorithms are plotted in figure 21, 22 and 23. Analyzing the graphs, the specificity performance is approximately equal results in our GHKF based road extraction algorithm when compared with other algorithms.

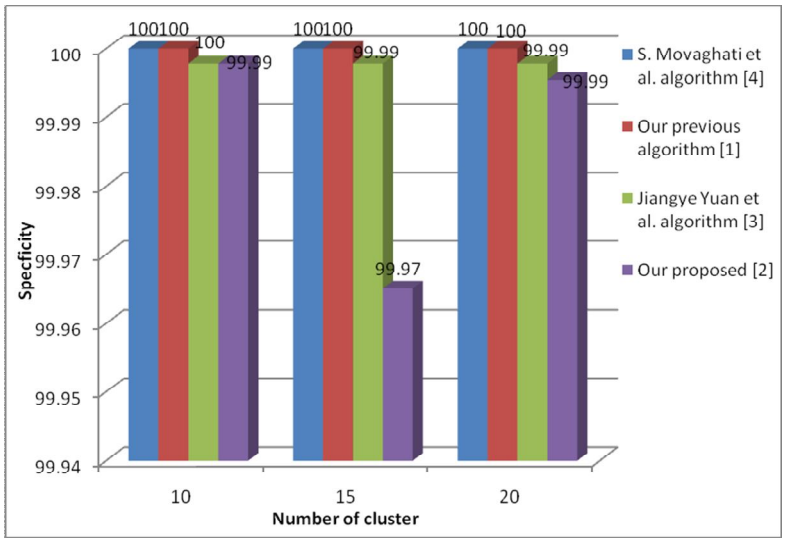

Fig 21: Specificity plot of comparative analysis for image 1

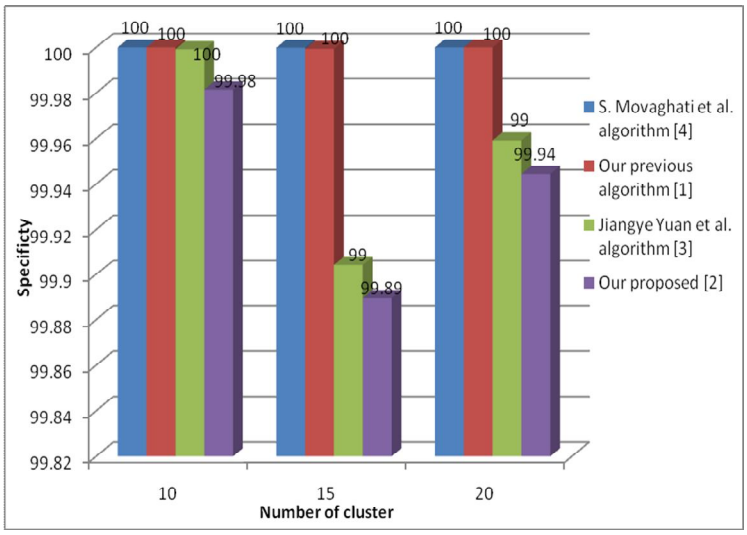

Fig 22: Specificity plot of comparative analysis for image 2

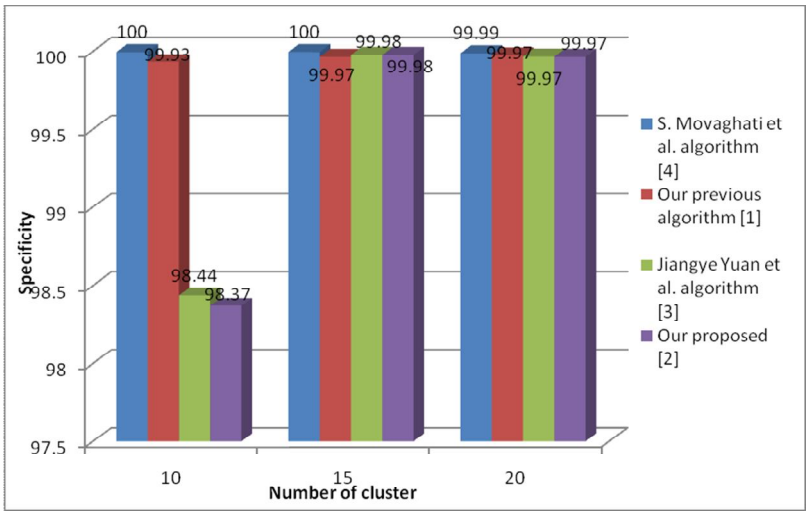

Fig 23: Specificity plot of comparative analysis for image 3

4. Conclusion

In this paper, we presented an extensive analysis of four road extraction algorithms done effectively. The performance study was carried out on four road extraction algorithms in terms of accuracy, completeness, correctness, sensitivity and specificity. Furthermore, the behavior of road extraction algorithm was analyzed with three satellite images. The comparative study has revealed that Gauss-Hermite Kalman Filter-Based Road Extraction algorithms such as our proposed [2], previous algorithm [1] achieved better accuracy when compared with other algorithms. The GHKF based proposed algorithm is efficient, reliable and it is able to process complicated satellite images from a variety of sources including urban areas from online maps.

References

[1] K. Madhan Kumar, R. Kanthavel,"Road Extraction from Satellite Images Using Unscented Kalman Filter and Gauss-Hermite Kalman Filter," International Review on Computers and Software (IRECOS), Vol. 8, No. 9, September 2013.

[2] K. Madhan Kumar, R. Kanthavel,A.Velayudham," Automatic Road Network Extraction through S-Legion and GHKF Using High Resolution Satellite Images", Information-An International Interdisciplinary Journal,Vol .17,No 9(B), September 2014

[3] Jiangye Yuan, DeLiang Wang,Bo Wu, Lin Yan, and Rongxing Li,"LEGION-Based Automatic Road Extraction From Satellite Imagery,"IEEE Transactions On Geo-science And Remote Sensing, Vol. 49, No. 11, November 2011.

[4] Movaghati, S., Moghaddamjoo, A., Tavakoli, A, "Road Extraction from Satellite Images Using Particle Filtering and Extended Kalman Filtering", IEEE Transactions on Geo-science and Remote Sensing, Vol. 48, No: 7, pp: 2807-2817, 2010.

[5] Alharthy, A., Bethel, J., "Automated road extraction from LIDAR data, "In: Proceedings of ASPRS Annual Conference, Anchorage, Alaska, Unpaginated CD-ROM, 2003.

[6] Choi, Y.W., Jang, Y.W., Lee, H.J., Cho, G.S.,"Heuristic road extraction," In: International Symposium on Information Technology Convergence, IEEE Computer Society, 2007.

[7] Clode, S., Rottensteiner, F., Kootsookos, P., Zelniker, E.,"Detection and vectorization of roads from LIDAR data," Photogrammetric Engineering and Remote Sensing, Vol.73, No.5, pp.517-536, 2007.

[8] Aluir P. Dal Poz, Rodrigo A. B. Gallis, and João F. C. da Silva, "Three-Dimensional Semiautomatic Road Extraction From a High-Resolution Aerial Image by Dynamic-Programming Optimization in the Object Space,"IEEE Geosciences And Remote Sensing Letters, Vol. 7, No. 4, October 2010.

[9] Jiuxiang Hu, Anshuman Razdan, John C. Femiani, Ming Cui, and Peter Wonka,"Road Network Extraction and Intersection Detection From Aerial Images by Tracking Road Footprints,"IEEE Transactions On Geoscience And Remote Sensing, Vol. 45, No. 12, December 2007.

[10] Jenita Subash and Madhan Kumar.K, "Road Tracking from High resolution IRS And IKONOS Images Using Unscented Kalman Filtering", International Journal of Electronic Signals and Systems,vol.1,no.1,pp.5-11.

[11] G. Vosselman and J. D. Knecht, "Road tracing by profile matching and Kalman filtering," in Proc. Workshop Autom. Extraction Man-Made Objects Aerial Space Images, Birkhaeuser, Germany, pp. 265–274, 1995.

[12] A. Baumgartner, S. Hinz, and C. Wiedemann, "Efficient methods and interfaces for road tracking," in Proc. Int. Arch. Photogram. Remote Sens, vol. 34, pp. 28–31, 2002.

[13] J. Zhou, W. F. Bischof, and T. Caelli, "Road tracking in aerial images based on human-computer interaction and Bayesian filtering," ISPRS J.Photogramm. Remote Sens., vol. 61, no. 2, pp. 108–124, 2006.

[14] M. Bicego, S. Dalfini, G. Vernazza, and V. Murino, "Automatic road extraction from aerial images by probabilistic contour tracking," in Proc.ICIP, pp. 585-588,2003.
[15] J.Mena, "State of the art on automatic road extraction for GIS update: A novel classification," Pattern Recognit. Lett, vol. 24, no. 16, pp. 3037-3058, 2003.
[16] Mckeown, D.Denlinger, J.L.,"Cooperative methods for road tracking in aerial imagery", In: Workshop Comput.Vision Pattern Recognition, pp.662-673, 1988.
[17] M. F. Auclair Fortier, D. Ziou, C. Armenakis, and S. Wang, "Automated correction and updating of roads from aerial ortho-images," in Proc. ISPRS, vol.33, pp.34-41, 2000.
[18] J. B. Mena, "State of the art on automatic road extraction for GIS update: A novel classification," Pattern Recognition. Lett. vol. 24, no. 16, pp. 3037-3058, 2003.
[19] M. Xia and B. Liu, "Image registration by super-curves," IEEE Trans. Image Process., vol. 13, no. 5, pp. 720–732, 2004.
[20] N. C. Rowe and L. L. Grewe, "Change detection for linear features in aerial photographs using edge-finding," IEEE Trans. Geosci. Remote Sens., vol. 39, no. 7, pp. 1608–1612, 2001.
[21] C. C. Chen, S. Thakkar, C. A. Knoblock, and C. Shahabi, "Automatically annotating and integrating spatial datasets," in Proc. Spatio-Temporal Database Manage, pp. 469–488, 2003.
[22] L. Bentabet, S. Jodouin, D. Ziou, and J. Vaillancourt, "Road vectors update using SAR imagery: A snake-based method," IEEE Trans. Geosci. Remote Sens., vol. 41, no. 8, pp. 1785-1803, 2003.
[23] F. Dell'Acqua and P. Gamba, "Detection of urban structures in SAR images by robust fuzzy clustering algorithms: The example of street tracking," IEEE Trans. Geosci. Remote Sens., vol. 39, no. 10, pp. 2287–2297, Oct. 2001.
[24] M. J. Song and D. Civco, "Road extraction using SVM and image segmentation," Photogramm. Eng. Remote. Sens., vol. 70, no. 12, pp. 1365–1371, Dec. 2004.
[25] W. Z. Shi and C. Q. Zhu, "The line segment match method for extracting road network from high-resolution satellite images," IEEE Trans. Geosci. Remote Sens., vol. 40, no. 2, pp. 511–514, Feb. 2002.
[26] P. Gamba, F. Dell'Acqua, and G. Lisini, "Improving urban road extraction in high-resolution images exploiting directional filtering, perceptual grouping, and simple topological concepts," IEEE Geosci. Remote Sens. Lett., vol. 3, no. 3, pp. 387–391, Jul. 2006.
[27] D. L. Wang and D. Terman, "Image segmentation based on oscillatory correlation," Neural Computation, vol.9, pp. 805-836, 1997.
[28] A. Baumgartner, C. Steger, H. Mayer, W. Eckstein, and H. Ebner, "Automatic road extraction based on multi-scale, grouping, and context," Photogramm. Eng. Remote Sens., vol. 65, no. 7, pp. 777-785, 1999.
[29] Rohit Maurya, Dr. Shalini Singh, Dr. P.R Gupta, and Manish Kumar Sharma," Road Extraction Using K-Means Clustering and Morphological Operations,"

International journal of advanced engineering sciences and technologies, Vol. 5, No. 2,pp.290-295,2011.

[30] Feng Jiang,Fuyang Chen,Changyun Wen, "Fuzzy Control for Road Intersection Signal with Bus Priority", Aloy Journal of Soft Computing and Applications (AJSCA), Volume 1 Issue 1, 2014.

K.Madhan Kumar (Karuppasamy Madhan Kumar) obtained his Bachelor's degree in Electronics and Communication Engineering (2001) from Manonmanium Sundaranar University. Then he obtained his Master's degree in Optical Communication (2004) from Anna University. Persuing PhD at Anna University, Chennai. He is a Life Member at ISTE professional Society. Currently, he is an Associate Professor at the Faculty of Electronics and Communciation Engineering, PET Engineering College Vallioor. His specializations include Optical communication, Microwave Engineering and Image processing. His current research interests are Remote sensing, satellite Image processing and Optical Networking.

Dr. R.Kanthavel (Radhakrishnan Kanthavel) received his Bachelor of Engineering Degree in Electronics & Communication Engineering in 1996. Then he obtained his Master of Engineering Degree in Communication Systems in 1999 from M.K University, India. He completed his Ph.D in Information and Communication Engineering from Anna University, Chennai. He is currently working as Professor & Head in the Department of Electronics and Communication Engineering at Velammal Engineering College, Chennai, affiliated to Anna University, Chennai. He has fifteen years teaching experience in various leading engineering colleges. He is a Life Member at ISTE, IEEE, IETE and CSI professional societies. He has published three books for engineering students. He has published more than twenty four research papers in reputed international and national journals. He has presented twenty research works in various international and national conferences. He is a reviewer in six international journals. His interests include Embedded Systems, Wireless Communication systems and Computer Networks.

A.Velayudham (Aiyappan Velayudham) is currently an Assistant Professor (Selection Grade) in the Department of Information Technology at Cape Institute of Technology, affiliated to Anna University, Chennai involving in research, teaching and administration activities. He received his B.E in Computer Science and Engineering from Manonmanium Sundaranar University in 2002 and M.E in Computer Science and Engineering from Annamalai University in 2004. Currently, he is pursuing his Ph.D Doctoral Research in Information & Communication Engineering from Anna University, Chennai. He is a Life Member at ISTE, IEEE and CSI professional societies. His specializations include Biometrics, Steganography & Neural Networks. He has published thirteen research papers in reputed international journals and twenty two research works in various international and national conferences. His current research interests are Image Processing, Medical Image Denoising & Soft Computing.